THE JOURNAL OF BIOLOGICAL CHEMISTRY VOL. 289, NO. 11, pp. 7399–7412, March 14, 2014

Wnt Protein-mediated Satellite Cell Conversion in Adult and Aged Mice Following Voluntary Wheel Running[S]

Received for publication, November 29, 2013, and in revised form, January 28, 2014 Published, JBC Papers in Press, January 30, 2014, DOI 10.1074/jbc.M113.539247

Shin Fujimaki[‡§1], **Ryo Hidaka**[‡1], **Makoto Asashima**[‡1], **Tohru Takemasa**[§2], **and Tomoko Kuwabara**[‡1,2,3]

From the [‡]*Research Center for Stem Cell Engineering, National Institute of Advanced Industrial Science and Technology, Tsukuba, Ibaraki 305-0046 and the* [§]*Physical Education, Health and Sport Sciences, Graduate School of Comprehensive Human Sciences, University of Tsukuba, Tsukuba, Ibaraki 305-8577, Japan*

Background: Satellite cells are activated in response to muscle injury or mechanical stimuli.
Results: Running-induced up-regulation of Wnt/β-catenin signaling activates *Myf5* and *MyoD* transcription.
Conclusion: Voluntary wheel running induces satellite cell activation by direct regulation of Wnt/β-catenin signaling.
Significance: Focusing on Wnt signaling may help to understand the function and intrinsic ability of satellite cells in adult myogenesis.

Muscle represents an abundant, accessible, and replenishable source of adult stem cells. Skeletal muscle-derived stem cells, called satellite cells, play essential roles in regeneration after muscle injury in adult skeletal muscle. Although the molecular mechanism of muscle regeneration process after an injury has been extensively investigated, the regulation of satellite cells under steady state during the adult stage, including the reaction to exercise stimuli, is relatively unknown. Here, we show that voluntary wheel running exercise, which is a low stress exercise, converts satellite cells to the activated state due to accelerated Wnt signaling. Our analysis showed that up-regulated canonical Wnt/β-catenin signaling directly modulated chromatin structures of both *MyoD* and *Myf5* genes, resulting in increases in the mRNA expression of *Myf5* and *MyoD* and the number of proliferative Pax7$^+$Myf5$^+$ and Pax7$^+$ MyoD$^+$ cells in skeletal muscle. The effect of Wnt signaling on the activation of satellite cells, rather than Wnt-mediated fibrosis, was observed in both adult and aged mice. The association of β-catenin, T-cell factor, and lymphoid enhancer transcription factors of multiple T-cell factor/lymphoid enhancer factor regulatory elements, conserved in mouse, rat, and human species, with the promoters of both the *Myf5* and *MyoD* genes drives the *de novo* myogenesis in satellite cells even in aged muscle. These results indicate that exercise-stimulated extracellular Wnts play a critical role in the regulation of satellite cells in adult and aged skeletal muscle.

Satellite cells are muscle-specific stem cells located between the basal lamina and plasma membrane of muscle fibers (1). In adult skeletal muscle, satellite cells represent the source of 2.5–6% of all the nuclei of a muscle fiber and remain in a quiescent state under normal conditions. Satellite cells play an essential role in muscle regeneration and recovery because they have the intrinsic ability to differentiate to generate a large number of new myofibers in few days (2). Exercise alters myofiber composition to increase muscle performance and metabolism and also has a positive effect on the regulation of satellite cells. Several studies have reported that the number of satellite cells increases after exercise in humans and animals (3, 4). In contrast, the number of satellite cells decreases during aging, and this is associated with a decrease in muscle quality and functional properties (5). Loss of skeletal muscle mass with concomitant fibrosis during aging eventually leads to sarcopenia. Sarcopenia is now recognized as a serious health issue affecting millions of aging adults, and exercise is one of the primary treatments used to prevent muscle shrinking and to reduce the risks of sarcopenia because it can increase muscle strength and endurance, even in old age.

Although physical exercise plays an important role in the intervention for sarcopenia, its effectiveness on satellite cells in the skeletal muscle during aging has not been well evaluated. Satellite cells exhibit a quiescent state and an activated proliferative state during skeletal muscle turnover, and each state can be identified with specific stage markers. Both quiescent and activated satellite cells express a stem cell-specific transcriptional factor, Pax7. Quiescent satellite cells are Pax7-positive but are negative for myogenic Myf5 and MyoD. In contrast, activated satellite cells co-express Myf5 and MyoD together with Pax7. Myf5 and MyoD are members of the basic helix-loop-helix transcriptional factors that play essential roles in controlling satellite cell differentiation and skeletal muscle development (6). Although changes in satellite cell numbers upon exercise stimulation have been extensively investigated, not many studies have been performed on the characteristic changes in satellite cells themselves, and the molecular mechanisms of exercise-stimulating extracellular factors controlling the expression profiles of satellite cells remain elusive.

Exercise alters various extracellular signals in skeletal muscles, affecting the fate of satellite cells. Wnt signaling during embryonic myogenesis and postnatal development plays important roles in lineage control (7). Wnt signaling

[S] This article contains supplemental Figs. S1 and S2.
[1] Supported by the National Institute of Advanced Industrial Science and Technology.
[2] Supported by a grant-in-aid for scientific research (B).
[3] Supported in part by a grant-in-aid for scientific research on innovative areas, The Takeda Science Foundation, and The Mitsubishi Foundation.
To whom correspondence should be addressed: Research Center for Stem Cell Engineering, National Institute of Advanced Industrial Science and Technology, Central 4, 1-1-4 Higashi, Tsukuba Science City, Ibaraki 305-8562, Japan. Tel.: 81-29-861-2529; Fax: 81-29-861-2897; E-mail: t.warashina@aist.go.jp.

induces satellite cell proliferation during skeletal muscle regeneration (8). The transition from Notch signaling to Wnt signaling controls the transition from proliferation to differentiation in myogenic progenitors during muscle regeneration (9). Wnt signaling has positive effects on skeletal muscle regeneration but negative effects related to the induction of muscle fibrosis (10). Although many studies have indicated that Wnt has multiple functions in skeletal muscle (10–13), the actions of Wnts in response to exercise stimuli have not been well characterized, especially their roles in the regulatory cascade with respect to controlling satellite cells.

Wheel running is an effective exercise model for long-distance running in rodents and is less stressful than other models because it is not a compulsive exercise (14, 15). Wheel running exerts various physiological effects, including decreased body mass, increased maximum oxygen uptake, and metabolic improvement of skeletal muscles (16–20). Remarkably, the number of satellite cells in skeletal muscle increases after wheel running (21). Although the molecular mechanism underlying this effect remains unclear, some studies have reported that Wnt signaling is activated by acute treadmill running and functional overload (22, 23). However, the contribution of Wnt/β-catenin signaling to the regulation of satellite cells in response to exercise is unknown, and parallel examinations of muscle fibrosis following exercise have not been performed.

In this study, we investigated the effects of Wnt/β-catenin signaling on the regulation of satellite cells after voluntary wheel running in both adult and aged mice. Interestingly, exercise significantly up-regulated the expression of *Wnt3*, *Wnt5a*, and *Wnt5b*, and the up-regulation of Wnt signaling altered the quiescent state of satellite cells into the activated state, even in aged skeletal muscle without fibrosis. Canonical Wnt signaling directly modulated the chromatin structures of the *Myf5* and *MyoD* promoters and up-regulated their expression in concert with the activation of satellite cells. To our knowledge, this report is the first to show the Wnt-mediated positive myogenic effects of exercise on satellite cells in adult and aged skeletal muscle and to describe the regulatory mechanism underlying chromatin remodeling of the *Myf5* and *MyoD* genes.

EXPERIMENTAL PROCEDURES

Animal Care—Animal experiments were carried out in a humane manner after receiving approval from the Institutional Animal Experiment Committee of the University of Tsukuba and the Institutional Animal Care and Use Committee (IACUC) of the National Institute of Advanced Industrial Science and Technology. Animals were housed in animal facilities with sufficiently controlled temperature and humidity under a 12/12-h light/dark cycle and had access to chow and water *ad libitum*. Male C57BL/6J mice (CLEA Japan, Japan) ages 8–12 weeks (adult) and 24 months (aged) were used in this study. To generate positive control samples of muscle injury, 100 μl of cardiotoxin (CTX,[4] 0.05 mg/ml; Sigma) was injected into the gastrocnemius in 12-week-old mice, and the gastrocnemius was excised 3 days after the injection.

Voluntary Wheel Running and Tissue Collection—Adult and aged mice were divided into a control group and runner group. Runner group mice were housed individually in cages (32 × 35 × 23 cm) equipped with a running wheel (16 cm in diameter) and performed voluntary wheel running for 4 weeks beginning at 8 weeks or 23 months of age. Wheel running activity was monitored continuously with an original program, which was used in our previous studies (24, 25). Daily and total running distances were recorded for each mouse throughout the duration of exercise. Each day at noon, running data were collected and recorded on the computer for each mouse, and the daily distance counter was reset. Control group mice were housed in cages without a running wheel. After 4 weeks of exercise, mice were sacrificed by cervical dislocation. For RNA isolation or protein extraction, the gastrocnemius muscles were dissected out quickly from each mouse. Each sample was then frozen in liquid nitrogen after measurement of the wet weight and kept in a freezer at −80 °C until homogenization. For immunohistochemistry, the chests of sacrificed mice were opened, and their tissues were fixed by circulation of PBS and then 4% paraformaldehyde throughout the body. The gastrocnemius muscles were then dissected from each mouse, and the samples were placed in 4% paraformaldehyde until analysis.

Immunohistochemical Analysis—Fixed samples were placed in a 30% sucrose solution and stored in the refrigerator overnight. Cross-sections were cut to a thickness of 200 μm using a microtome (ROM-380, Yamato Kohki) and stored in tissue collection medium (25% glycerin, 30% ethylene glycol, 0.05 M phosphate) at −20 °C until analysis. We verified that there were no differences between the sections cut after fixation and the frozen sections (data not shown). For pretreatment for the staining of 5-bromo-2′-deoxyuridine (BrdU), sections were incubated in 50% formaldehyde for 90 min at 65 °C. After washing with Tris-buffered saline containing 0.25% Triton X-100 (TBS-T), sections were incubated in 1 N HCl for 15 min at 37 °C. Sections were then incubated in 0.1 M borate buffer, pH 8.5, for 10 min at room temperature.

Sections were washed carefully, permeabilized with TBS-T, and blocked with 5% normal donkey serum in TBS for immunofluorescent staining. The primary antibodies used in this study included the following: mouse anti-Pax7 (1:10, Developmental Studies Hybridoma Bank); rabbit anti-Myf5 (1:200, Abcam, Tokyo, Japan), rabbit anti-MyoD (1:200, Santa Cruz Biotechnology); rat anti-BrdU (1:250, Abcam); rat anti-ER-TR7 (1:500, Abcam); rabbit anti-dystrophin (1:200, GeneTex); goat anti-Wnt3 (1:300, Everest Biotech Ltd., Oxfordshire, UK); rabbit anti-periostin (1:500, Abcam); mouse anti-myosin heavy chain 2a (1:20, Developmental Studies Hybridoma Bank), and rabbit anti-collagen 1 (1:200, Abcam). Sections were incubated for 3 days at 4 °C. For secondary detection, Cy3-conjugated donkey anti-rabbit, -rat, or -goat IgG (1:500, Jackson ImmunoResearch), Cy5-conjugated donkey anti-rat IgG (1:500, Jackson ImmunoResearch), and AlexaFluor 488-conjugated donkey anti-mouse or -rabbit IgG (1:500, Invitrogen) were used with DAPI (Wako, Osaka, Japan), and sections were incubated overnight at 4 °C. After several careful washes, sections were placed on glass slides and enclosed using

[4] The abbreviations used are: CTX, cardiotoxin; GSK-3β, glycogen synthase kinase β; HDAC1, histone deacetylase 1; LEF, lymphoid enhancer factor; p70S6K, p70 S6 kinase; TCF, T-cell factor; qRT, quantitative RT; IHC, immunohistochemistry.

TABLE 1
Primer sequences for qRT-PCR

Target gene	Sequence (5′–3′)	Product length
		bp
GAPDH		
Forward	GTATGTCGTGGAGTCTACTG	157
Reverse	CTTGAGGGAGTTGTCATATTTC	
IL-6		
Forward	CTCTGCAAGAGACTTCCATCCA	92
	AGTCTCCTCTCCGGACTTGT	
TNF-a		
Forward	ATGGCCTCCCTCTCATCAGT	105
Reverse	CTTGGTGGTTTGCTACGACG	
Pax7		
Forward	AAATCCGGGACCGGCTGCTGAA	196
Reverse	AGACGGTTCCCTTTGTCGCCCA	
Myf5		
Forward	AGGAATGCCATCCGCTACAT	141
Reverse	GTTACATTCAGGCATGCCGT	
MyoD		
Forward	GGATGGTGTCCCTGGTTCTTCAC	140
Reverse	CTATGTCCTTTCTTTGGGGCTGGA	
Myog		
Forward	AACTACCTTCCTGTCCACCTTCA	110
Reverse	GTCCCCAGTCCCTTTTCTTCCA	
HeyL		
Forward	GGCACAGGGTTCTTTGATGC	165
Reverse	TGCATAGCTCTTGAGGTGGG	
DLL4		
Forward	ACAAGAATAGCGGCAGTGGTCGCA	179
Reverse	ACCCACAGCAAGAGAGCCTTGGATG	
Wnt3		
Forward	GCCACAACACGAGGACGGAGAAAC	151
Reverse	CCGCACAATCTACCCCTTCCCAGT	
Wnt5a		
Forward	GACTATGGCTACCGCTTCGC	164
Reverse	TGACACTTACAGGCTACATCTGC	
Wnt5b		
Forward	CAGGGCATTGGGATGGGTTGAG	185
Reverse	AGGAAGTTGGCTGCACACGG	
TGF-b		
Forward	GCTGAACCAAGGAGACGGAA	138
Reverse	ATGTCATGGATGGTGCCCAG	
Col1a2		
Forward	GATGGTCAGCCTGGACACAA	199
Reverse	GGATGCCTTGAGGACCACTA	
Col5a3		
Forward	AGCCAGCCAATCAGTCTGTC	149
Reverse	GTGCCACCTGCCATCCATAA	
Fn1		
Forward	TTACCAACCGCAGACTCACC	88
Reverse	CCACTGCATTCCCACAGAGT	
Postn		
Forward	ATGCCTTACACAGCCACATG	147
Reverse	TGACTCGAGCACAGTTCACA	

mounting medium (Vectashield; Vector Laboratories, Burlingame, CA). The images were analyzed using an Olympus FV1000-D confocal microscope (Olympus Corp., Tokyo, Japan).

RNA Isolation and Quantitative RT-PCR (qRT-PCR) Analysis—Total RNA was isolated from frozen muscle tissues using Isogen. RNA samples were treated with Turbo DNase to remove genomic DNA. cDNA synthesis was performed using PrimeScript RT Master Mix (TaKaRa Bio., Otsu, Japan) according to the manufacturer's recommendations. Synthesized cDNA was diluted 10-fold with diethylpyrocarbonate (DEPC) water and used as real time PCR samples. qRT-PCR was performed using Thunderbird SYBR qPCR Mix (Toyobo, Osaka, Japan) and a CFX96 real time PCR system (Bio-Rad). In this study, we used sets of primers synthesized by Invitrogen (Table 1). The PCR protocol was as follows: denaturing for 15 s at 95 °C, annealing and extension for 40 s at 60 °C, 40 cycles. The dissociation curve for each sample was analyzed to verify the specificity of each reaction. The relative mRNA expression levels of target genes was determined by the $\Delta\Delta Ct$ method and normalized to the expression of *GAPDH*. We confirmed that there were no differences between the data determined by the $\Delta\Delta Ct$ method and the standard curve method (data not shown).

Protein Extraction and Western Blot Analysis—Each tissue was homogenized in lysis buffer (50 mM Hepes, pH 7.4, 150 mM NaCl, 10 mM EDTA, 10 mM NaF, 10 mM $Na_4P_2O_7$, 2 mM Na_3VO_4, 1% sodium deoxycholate, 1% Nonidet P-40, 0.2% SDS) with protease inhibitor mix (4-(2-aminoethyl)benzenesulfonyl fluoride, aprotinin, E-64, leupeptin hemisulfate monohydrate, bestatin, pepstatin A; Nacalai Tesque, Kyoto, Japan) on ice. Homogenates were then centrifuged at 1,770 × *g* for 10 min at 4 °C, and the supernatants were collected. After measurement of the protein concentrations using a BCA protein assay kit (Thermo Fisher Scientific, Yokohama, Japan), samples were normalized to 2 μg/μl with SDS-PAGE loading buffer (62.5 mM Tris-HCl, pH 6.8, 2% w/v SDS, 10% glycerol, 50 mM DTT, 0.01% w/v bromphenol blue). Protein extractions were run on SDS-polyacrylamide gels (SuperSep Ace, Wako) and transferred to polyvinylidene difluoride membranes. Membranes were blocked in Blocking One (Nacalai Tesque) for 1 h at room temperature. The primary antibodies used were obtained from Cell Signaling Technology (Danvers, MA) and included the following: rabbit anti-Akt (1:1,000); rabbit anti-phospho-Akt (Ser-473; 1:1,000); rabbit anti-p70S6K (1:1,000); rabbit anti-phospho-p70S6K (Thr-389; 1:500); rabbit anti-GSK-3β (1:2,000); rabbit anti-phospho-GSK-3β (Ser-9; 1:2,000); rabbit anti-β-catenin (1:2,000); and from Santa Cruz Biotechnology included the following: rabbit anti-Myf5 (1:200); rabbit anti-MyoD (1:200), and rabbit anti-GAPDH (1:2,000). Membranes were incubated overnight at 4 °C. Anti-rabbit IgG, HRP-linked whole anti-donkey (1:20,000, GE Healthcare), was used as a secondary antibody, and membranes were incubated for 1 h at room temperature. After careful washes in TBS containing 0.05% Tween 20, membranes were soaked in Pierce Western Thermo blotting substrate (Thermo Fisher Scientific), and the bands were visualized using a chemiluminescence system and an LAS-3000 Mini luminescent image analyzer (FUJIFILM, Tokyo, Japan). Images for each membrane were analyzed using ImageJ software (National Institutes of Health; rsbweb.nih.gov) as described previously (26). Average and standard deviations were calculated based on the signal intensities from each experiment. Myf5, MyoD, and β-catenin immunoreactivity was normalized to that of GAPDH.

Chromatin Immunoprecipitation (ChIP) Assay—Approximately 20–50 μg of DNA from each muscle sample was used to perform chromatin immunoprecipitation (ChIP). The following primary antibodies were used for the ChIP assay: rabbit antibody to β-catenin (Sigma), rabbit antibody to histone deacetylase 1 (HDAC1, Millipore, Billerica, MA), rabbit antibody to LEF1 (Millipore, rabbit antibody to TCF), and mouse antibody to heterochromatin protein 1 (HP1) (Millipore). Normal rabbit IgG was used as a negative control in the analysis. Normal rabbit IgG and anti-acetylated histone H3 were obtained from Millipore. The acetylated histone H3 antibody detects diacetylation at lysines 9 and 14. Anti-H3K9me2 and anti-H3K4me2 were also obtained from Millipore.

ChIP was performed using a commercial kit (Millipore) according to the manufacturer's recommendations. Briefly, chromatin was precleared with a protein A-agarose slurry with salmon sperm DNA by incubation for 1 h at 4 °C on a rotating platform in a volume of ~1 ml with ChIP dilution buffer (0.01% SDS, 1.1%, Triton X-100, 1.2 mM EDTA, 16.7 mM Tris-HCl, pH 8.1, and 167 mM NaCl). After agarose removal by centrifugation, 1% of the precleared chromatin was saved and used as input DNA. Antibodies were added to the chromatin and incubated at 4 °C with rotation for 1 h. Immunoprecipitation was performed with 1.0 μg of antibodies. Protein A-agarose was added and incubated at 4 °C with rotation for 2 h. Three separate washes with low salt immune complex wash buffer (0.1% SDS, 1% Triton X-100, 2 mM EDTA, 20 mM Tris-HCl, pH 8.1, and 150 mM NaCl) were then performed, followed by separate washes for 15 min with rotation with the following buffers: high salt immune complex wash buffer (0.1% SDS, 1% Triton X-100, 2 mM EDTA, 20 mM Tris-HCl, pH 8.1, and 500 mM NaCl); LiCl salt immune complex buffer (0.25 M LiCl, 1% Igepal-CA630, 1% deoxycholic acid (sodium salt), 1 mM EDTA, and 10 mM Tris, pH 8.0); and two separate washes with TE buffer (10 mM Tris-HCl, 1 mM EDTA, pH 8.0). Chromatin·DNA complexes were eluted (0.1 M $NaHCO_3$, 1% SDS) from agarose beads, and cross-links were reversed by incubation at 65 °C for 4 h. Samples were RNase-treated (RNase A); protein was digested (proteinase K), and DNA was purified using a spin column (Wizard DNA clean-up system, Promega). Immunoprecipitated DNA for specific genes was analyzed and quantified by PCR. PCR primers used with ChIP samples were as follows: *Myf5* promoter 2.4 kb upstream (forward, 5′-TGTGTGGACAAGGGTAAATTA-3′; reverse, 5′-CACCATCTTCACAGAGTAA-CT-3′) and *MyoD* promoter 2.7 kb upstream (forward, 5′-CTTTACACTTCCACC-TGAATG-3′; reverse, 5′-AGGGACATTAAAGATCGCTTT-3′). The number of PCR cycles and amount of ChIP DNA were adjusted so that the accumulated product was in the linear range of the exponential curve of the PCR amplifications. PCR products were separated by electrophoresis on agarose gels and stained with Gel Green (Biotium Inc.). The ultraviolet light-induced fluorescence of stained DNA was captured by a Dolphin-View2 imaging system (Kurabo, Osaka, Japan), and intensities of the signals were quantified by ImageJ software, as described previously (26). For each threshold, multiple independent ChIP experiments were performed. Average and standard deviations were calculated based on the signal intensities from each experiment.

Statistical Analysis—Experiments were analyzed for statistical significance using a Student's *t* test, with all error bars expressed as means ± S.D. Differences with *p* values of less than 0.05 were considered significant.

RESULTS

Voluntary Wheel Running Provided Mild Stimulation for the Gastrocnemius Muscle—Adult and aged mice performed voluntary wheel running for 4 weeks (Fig. 1*A*). The running distances were ~13 km/day for adult mice and ~4 km/day for aged mice. There were no changes in body mass or wet weight of gastrocnemius muscles after 4 weeks of running in both adult and aged mice (Fig. 1*B*). In previous studies of high intensity exercise, such as functional overload leading to muscle hypertrophy, Akt/mammalian target of rapamycin/p70S6K signaling is activated in skeletal muscle to increase the levels of cellular protein synthesis (27, 28). In contrast, in voluntary wheel running, a low intensity exercise without excessive stress, the activation levels of Akt/mammalian target of rapamycin/p70S6K signaling components were relatively low (Fig. 1*C*). Akt and p70S6K phosphorylation did not change after running, indicating that voluntary wheel running was only a mild physiological stimulus in this study.

Several studies have demonstrated that high intensity exercise also induces muscle inflammation involving acute muscle regeneration, as shown by increases in tumor necrosis factor-α (*TNF-α*) and interleukin-6 (*IL-6*) mRNA expression in skeletal muscle (29–32). However, in this study, activation of these typical inflammatory signals and cytokines was not detected, and *TNF-α* and *IL-6* mRNA expression levels were normal. Although *TNF-α* and *IL-6* mRNA expression levels were slightly up-regulated after exercise in both adult and aged runner mice, the fold change was significantly lower than that of the positive control, in which up-regulation of inflammatory cytokines was induced via muscle injury (*i.e.* injection of CTX; Fig. 1*D*). These results indicated that voluntary wheel running induced neither dynamic changes in the activities of protein synthesis signaling nor acute exercise-associated inflammation in both adult and aged skeletal muscle after 4 weeks of running.

Voluntary Wheel Running Activated Satellite Cells and Proliferation in Both Adult and Aged Skeletal Muscle—Satellite cells express Pax7 as a master transcription factor in the skeletal muscle lineage. Unlike the quiescent population, activated satellite cells co-express Myf5 and MyoD together with Pax7. Although it is well known that the number of satellite cells increases following wheel running in adult skeletal muscle, detailed characterization of the stages of these induced satellite cells and parallel examinations in both adult and aged animals have not been investigated. Our study indicated that the number of $Pax7^+$ cells increased following wheel running in both adult and aged mice (data not shown), being consistent with a previous report (21). The number of $Pax7^+$ cells increased more than 3-fold in adult mice and 2-fold in aged mice following 4 weeks of voluntary wheel running. Notably, in the case of aged mice (2 years old), exercise rescued the decrease in the number of $Pax7^+$ cells during aging, and the number of increased $Pax7^+$ cells was almost the same as that in adult mice at 12 weeks of age. Because $Pax7^+$ cells include both quiescent and activated satellite cell populations, immunohistochemical analysis using muscle cross-sections was performed to determine how the satellite cell population changes after running. In adult mice, although $Pax7^+MyoD^+$-activated satellite cells were rarely observed in the control group, $Pax7^+MyoD^+$-activated satellite cells clearly appeared in the runner group (Fig. 2*A*). Similarly, in aged mice, activated satellite cells significantly increased in the runner group (Fig. 2*B*). The number of $Pax7^+MyoD^+$ cells increased following running by nearly 6-fold, even in aged mice. Our immunohistochemistry (IHC) analysis suggested that mild running exercise effectively increased the number of satellite cells and that the increased population was predominantly characterized by activated satellite cells rather than quiescent satellite cells.

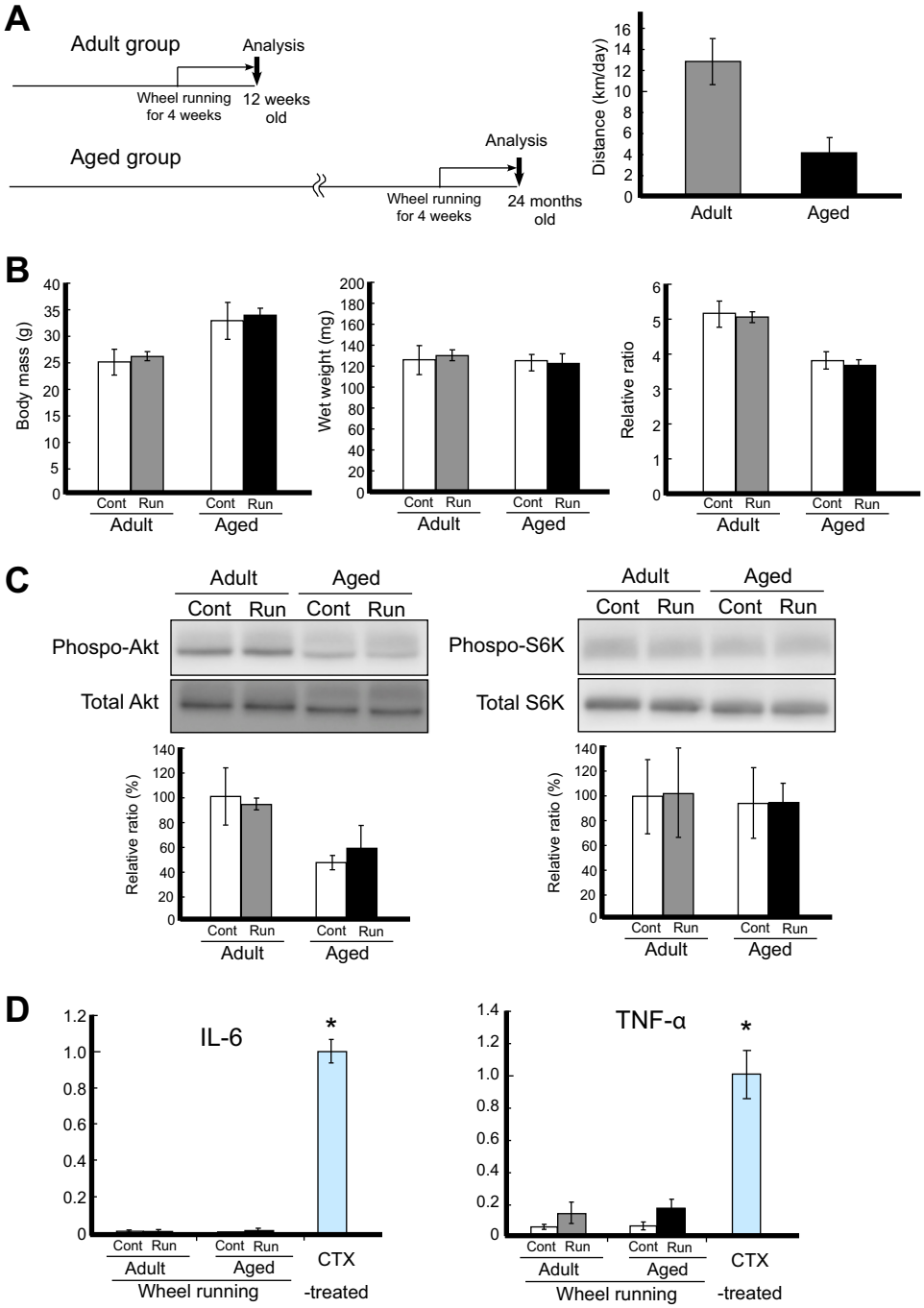

FIGURE 1. **Mild stimulation of the gastrocnemius by voluntary wheel running.** *A,* schematic representation of the experimental design in the runner group. Adult mice performed wheel running from 9 to 12 weeks of age and aged mice performed from 23 to 24 months of age. *B,* changes in body mass and muscle weight after exercise. The body mass (g), wet weight (mg) of gastrocnemius, and the relative ratio (mg/g) in each group were plotted. The relative ratio of the wet weight against the body mass is shown. *C,* representations of Akt (Ser-473) phosphorylation levels (*left*) and p70S6K (Thr-389) phosphorylation levels (*right*), as detected by Western blot analysis. Phosphorylation levels were calculated to divide the signal of the phosphorylated form against the total protein expression for Akt or S6K. The relative ratio, normalized to the signal observed for the control (*Cont*) adult group, is shown (*bottom graph*). *D,* expression levels of inflammatory markers (*IL-6*, *left*; *TNF-α*, *right*). The amounts of each mRNA in the gastrocnemius were measured by qRT-PCR analysis. As a positive control, the expression level in muscles injected with CTX, which induces remarkable muscle injury, was used in the analysis. The relative ratio of expression normalized to expression levels in CTX-treated muscle is shown. Signals are represented by *white bars* (controls in adult and aged mice), *gray bars* (adult runner mice), and *black bars* (aged runner mice). Values are expressed as the mean ± S.D. ($n = 4$/group). Significant differences are as follows: *, compared with all other groups ($p < 0.05$).

We next examined the effects of exercise on BrdU incorporation to satellite cells in skeletal muscle using $Pax7^+Myf5^+$ staining. The mitotic marker BrdU was administered daily during the last week of the exercise period. The number of $BrdU^+$ cells increased more than 2-fold after running in adult and aged mice (data not shown), indicating that exercise stimulated cellular proliferation, consistent with the results of a previous study (33). Importantly, the proportion of $Pax7^+Myf5^+BrdU^+$ and $Pax7^+MyoD^+BrdU^+$ cells to total $Pax7^+$ cells significantly increased after running (Fig. 2, *C* and *D*). Because $BrdU^+$ cells

indicate proliferating and newly generated cell populations, $Pax7^+Myf5^+BrdU^+$ cells and $Pax7^+MyoD^+BrdU^+$ cells represented proliferating activated satellite cells.

Because of the finding of *de novo* proliferative population within activated satellite cells during IHC analysis, we performed qRT-PCR analysis to confirm and compare the expression levels of the stem cell marker genes *Pax7*, *Myf5*, and *MyoD* using skeletal muscle-derived total RNAs in samples from both adult and aged mice. Unexpectedly, the mRNA expression levels of *Pax7* were not altered in the adult mouse group (Fig. 2*E*,

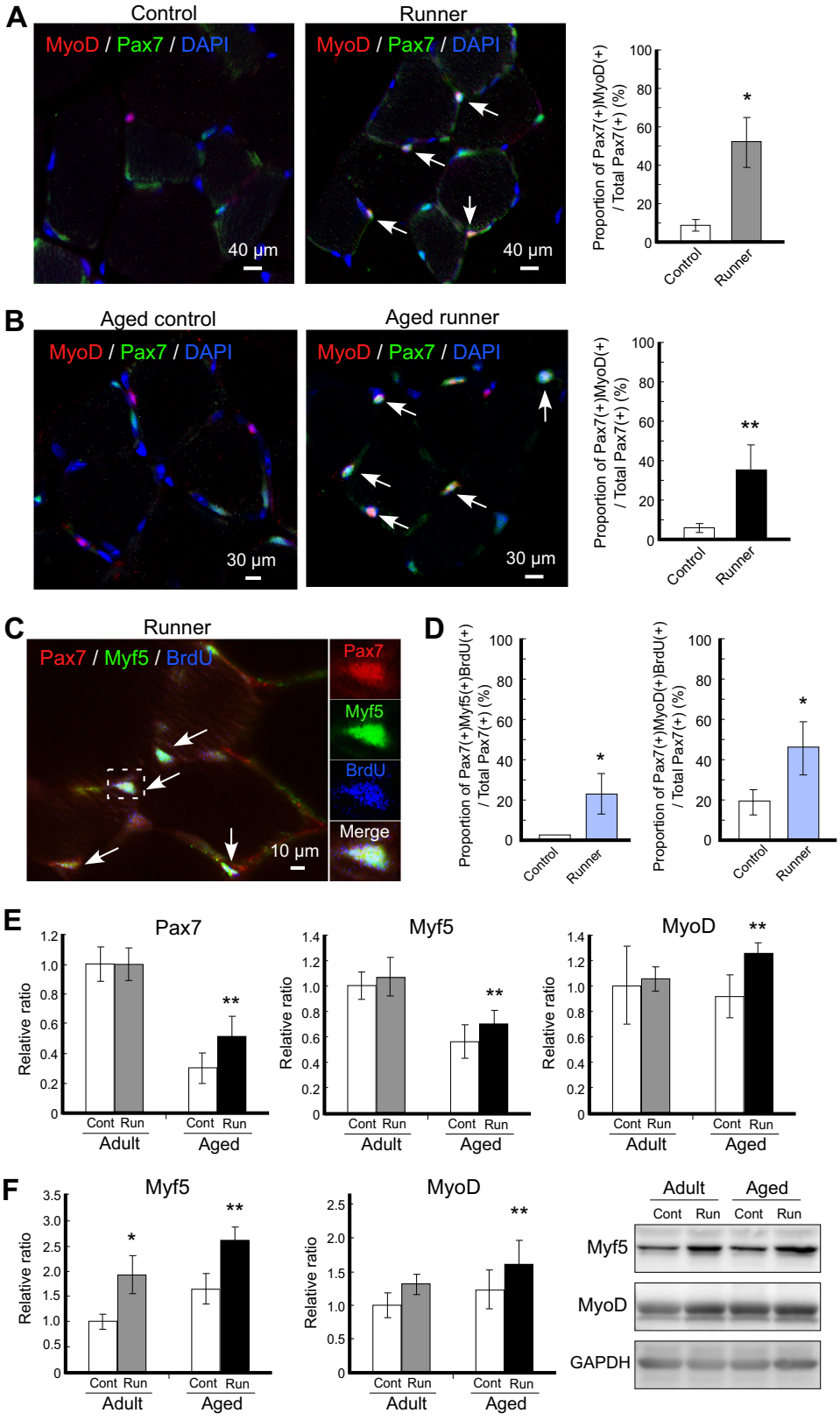

left panel), suggesting that the observation of increased numbers of $Pax7^+$ cells following voluntary running exercise reflected changes in protein levels only and did not induce dramatic changes in transcription in adult mice. However, *Pax7* mRNA expression was significantly elevated by exercise in the aged mouse group (Fig. 2*E*, *left panel*). Furthermore, the *Myf5* and *MyoD* genes tended to up-regulate in adult mice and were significantly up-regulated in aged mice following exercise (Fig. 2*E*, *middle* and *right panels*), and these data are consistent with protein levels by Western blot analysis (Fig. 2*F*). These data suggested that the relatively high levels of up-regulation of the *Myf5* and *MyoD* genes compared with that of the *Pax7* gene may contribute to the population change within $Pax7^+$ satellite cells from the quiescent state into the activated state. Additionally, the observation of changes in *Myf5* and *MyoD* mRNA levels in both adult and aged runner mice and the new production of $Pax7^+Myf5^+BrdU^+$ and $Pax7^+MyoD^+BrdU^+$ cells after exercise led us to consider the regulatory link between transcriptional control of the myogenic *Myf5* and *MyoD* genes and extracellular signals stimulated by voluntary wheel running.

Voluntary Wheel Running Activated Canonical Wnt/β-Catenin Signaling—To examine the molecular mechanisms underlying satellite cell activation after running, we focused on the Notch and Wnt signaling pathways, which regulate satellite cell self-renewal and myogenesis at the developmental embryonic stage (34). The expression of Delta ligand 4 (*DLL4*) and *HeyL*, which are the ligand and target gene, respectively, in Notch signaling, tended to decrease slightly after exercise in both the adult and aged groups (Fig. 3*A*). Although Notch signaling plays a critical role in controlling the proliferation of satellite cells in their lineage, the decreased expression of the ligand and target gene in our analysis implied that the generation of activated satellite cells via voluntary exercise, and the transcriptional control of the *Myf5* and *MyoD* genes was probably unrelated to the Notch pathway.

Wnts are extracellular ligands that modulate the cell fate choice event of various types of adult stem cells (35–37). As a paracrine factor, the stem cell niches express Wnts by responding to external stimuli (38, 39). In adult skeletal muscles following exercise, Wnt3 ligand was produced from myofibers rather than undifferentiated satellite cells (data not shown); therefore, we analyzed further the expression profiles of Wnt proteins using whole muscle tissue. Interestingly, the expression of Wnt ligands (*Wnt3*, *Wnt5a*, and *Wnt5b)* significantly increased after mild exercise, and their up-regulation was consistently observed in both the adult and aged runner groups (Fig. 3*B*). The expression of *Wnt3* increased more than 3-fold in adult mice and 2-fold in aged mice after 4 weeks of voluntary wheel running, and the promotional effect was consistent with the increase in $Pax7^+MyoD^+$-activated satellite cells in adult and aged runner mice. Wnt signaling plays an important role in further promoting myogenic differentiation in lineage-committed progenitor cells but not in undifferentiated satellite cells in which Notch signaling retains fate control under normal physiological conditions (9). In Wnt signaling, there are canonical and noncanonical signaling routes that depend on the type of Wnt protein, with Wnt3 being canonical signaling members that transduce their signals through intracellular β-catenin. Although Wnt5a and Wnt5b are included in noncanonical signaling members, Wnt5a has been reported to regulate the accumulation of β-catenin in a previous study (8). In fact, the expression of *Wnt5a* and *Wnt5b* was increased after running, consistent with *Wnt3* expression (Fig. 3*B*). Thus, we supposed that Wnt5a and Wnt5b have the function as canonical signaling members. The noncanonical Wnt signaling pathway has been found to be associated with myogenic regulation in skeletal muscle (7).

Next, we evaluated intracellular signal transduction because the Wnt member proteins Wnt3, Wnt5a, and Wnt5b were obviously associated with the promotion of activated satellite cells upon exercise. The phosphorylation of glucose synthase kinase 3β (GSK-3β) and β-catenin was investigated by Western blot analysis (Fig. 3*C*). β-Catenin, which acts in the nucleus with TCF and LEF transcriptional factors, is phosphorylated by GSK-3β, which leads to its ubiquitin-dependent degradation in the absence of Wnt ligands (43). However, when Wnt binds to the frizzled receptor, GSK-3β is phosphorylated (and therefore inactivated), and β-catenin accumulates and can translocate into the nucleus to activate its target genes. The phosphorylation of GSK-3β (Ser-9) tended to increase, and the expression of β-catenin significantly increased after voluntary running in both adult and aged mice, indicating that canonical Wnt/β-catenin signaling was activated upon performing exercise. Based on these results, our data confirmed that voluntary wheel running induced the activation of satellite cells, the activation of *Myf5* and *MyoD* transcription, the expression of canonical Wnt member proteins, and the activation of canonical Wnt/β-catenin signaling in both adult and aged skeletal muscle.

Voluntary Running-dependent Wnt Activation Did Not Induce Skeletal Muscle Fibrosis—Next, we investigated how fibrosis was related to elevated Wnt/β-catenin levels in the skeletal muscle after a voluntary running exercise. IHC analysis using antibodies against ER-TR7, a specific marker of reticular fibroblasts and reticular fibers, and the plasma membrane marker dystrophin showed that there were no significant differences between the control group and runner group in both

FIGURE 2. **Activation of satellite cells following voluntary wheel running.** *A* and *B,* immunohistochemistry analysis of satellite cells following exercise. Representative merged images of immunohistochemistry staining for MyoD (*red*) and Pax7 (*green*) with DAPI from adult (*A*) and aged mice (*B*) are shown. *Left panels* are from the control group, and *right panels* are from the runner group. The proportions of $Pax7^+MyoD^+$ cells per total $Pax7^+$ cells are shown in the *right graph*. *White arrows* indicate $Pax7^+MyoD^+$ cells. *C,* representative merged images of immunohistochemistry staining for Pax7 (*red*), Myf5 (*green*), and BrdU (*blue*) from the adult runner group. Magnification of the area surrounded by the *dashed square* is shown in the *right panels*, and *white arrows* indicate $Pax7^+MyoD^+BrdU^+$ cells. *D,* proliferative activated satellite cells increased following exercise. The proportion of $Pax7^+MyoD^+BrdU^+$ cells per total $Pax7^+$ cells in each group was plotted. *E* and *F,* expression profiles of stem cell markers of satellite cells. The mRNA expression levels of satellite cells markers (*Pax7*, *left*; *Myf5*, *center*; *MyoD*, *right*) in gastrocnemius were detected by qRT-PCR (*E*). The protein expression levels of Myf5 (*left graph*) and MyoD (*right graph*) in gastrocnemius were detected by Western blot. The *right images* represent the typical blot patterns of Myf5 (*upper*), MyoD (*middle*), and GAPDH (*lower*) (*F*). In all graphs, signals are represented by *white bars* (controls (*Cont*) in adult and aged mice), *gray bars* (adult runner (*Run*) mice), and *black bars* (aged runner mice). The mRNA and protein values were normalized to that of GAPDH and then plotted as the expression ratio relative to the control sample in adult mice. All data are expressed as the mean ± S.D. ($n = 4$/group). Significant differences are as follows: *, compared with adult control group; **, compared with aged control group ($p < 0.05$).

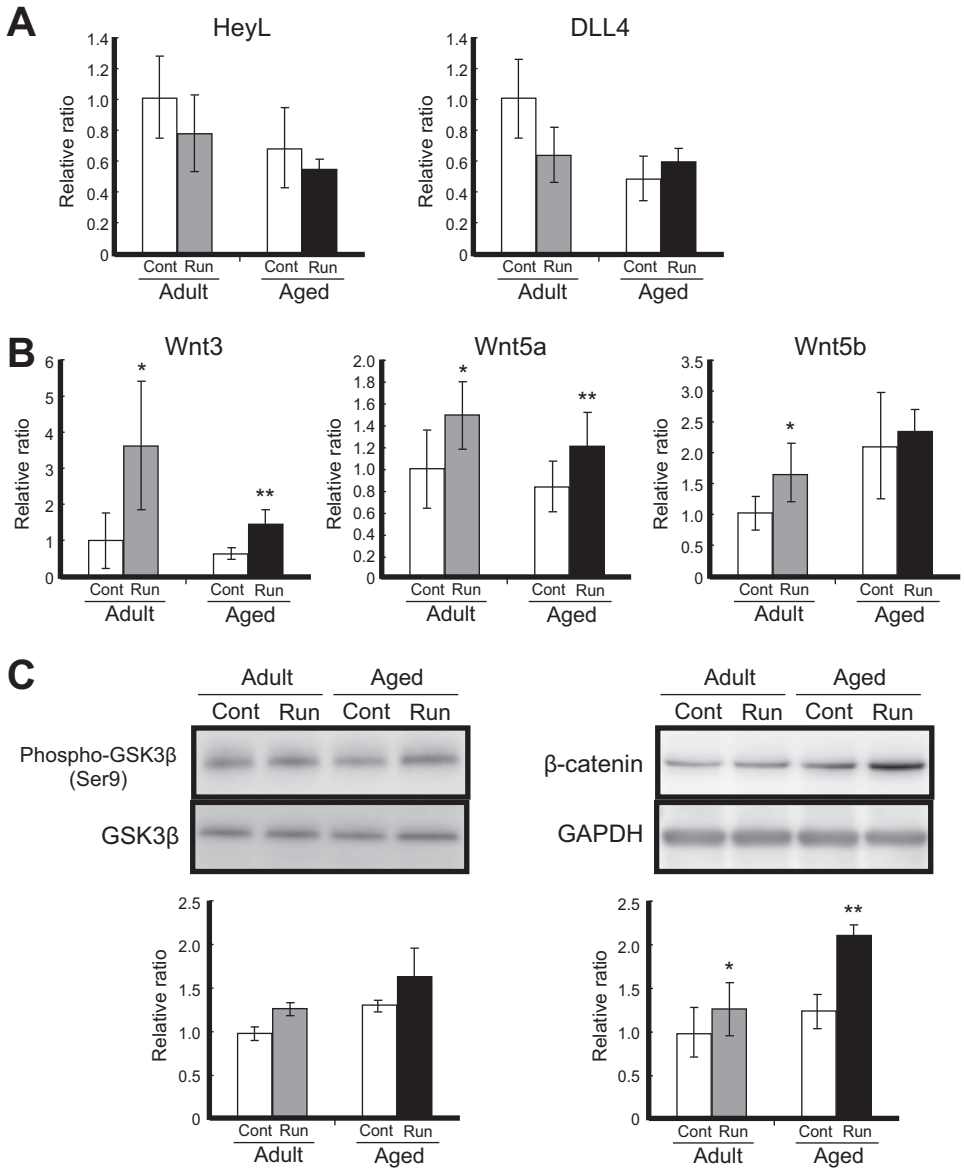

FIGURE 3. **Up-regulation of Wnt/β-catenin signaling following voluntary wheel running.** *A,* expression levels of Delta ligand 4 (*DLL4*) and *HeyL* mRNAs. Amounts of *DLL4* and *HeyL* mRNAs in the gastrocnemius were measured by qRT-PCR analysis. Target mRNA expression was normalized to that of *GAPDH* and then plotted as the expression ratio relative to the control sample in adult mice. *B,* expression levels of *Wnt3*, *Wnt5a*, and *Wnt5b* mRNAs in the gastrocnemius. *C,* Western blot analysis of GSK-3β phosphorylation (Ser-9; *left*) and accumulated β-catenin (*right*). *White bars,* controls (*Cont*) in adult and aged mice; *gray bars*, adult runner (*Run*) mice; *black bars,* aged runner mice. All data are shown as the relative ratio (normalized to the adult control group) and expressed as the mean ± S.D. ($n = 4$/group). Significant differences are as follows: *, compared with adult control group; **, compared with aged control group ($p < 0.05$).

adult and aged mice (Fig. 4, *A* and *B*). IHC analysis using antibodies against periostin (Postn), a matricellular fibrotic protein, and MHC2a provided similar results, with no fibrotic features in all skeletal muscle tissues examined (Fig. 4*C*). Activated satellite cells first differentiate into myoblasts and then into myocytes (myogenin-positive cells), finally giving rise to myofibers (expressing MHC). Wheel running usually produces a shift from type 2b (glycolytic fiber) MHC isoforms to type 2a (oxidative fiber) MHC isoforms in skeletal muscle (19). Clear changes were observed in MHC2a$^+$ fibers in the runner group, with an increase observed in the MHC2a$^+$ population following wheel running in both adult and aged skeletal muscle, indicating the occurrence of exercise-mediated oxidative metabolism (Fig. 4*C*). However, the expression of Postn was unchanged after running, suggesting that fibrosis was not promoted by exercise. Further IHC analysis using antibodies against collagen 1 showed no differences between the control and runner groups in adult and aged mice (data not shown). Additionally, qRT-PCR analysis of the genes associated with muscle fibrosis (*i.e.* TGF-β, collagen 1α2 (*Col1a2*), collagen 5α3 (*Col5a3*), fibronectin (*Fn1*), and *Postn*) confirmed that elevated Wnt expression in the skeletal muscle due to exercise was not correlated with fibrosis because almost no changes were observed in the expression levels of fibrosis-associated genes (Fig. 4*D*). Taken together, these data demonstrated that activation of Wnt/β-catenin signaling after voluntary running did not cause fibrosis, even in aged skeletal muscle.

Up-regulated Wnt/β-Catenin Signaling Regulated Satellite Cell Activation—Our analysis indicated that 4 weeks of voluntary wheel running efficiently promoted the expression of *Wnt3, Wnt5a*, and *Wnt5b*, even in aged skeletal muscle (Fig.

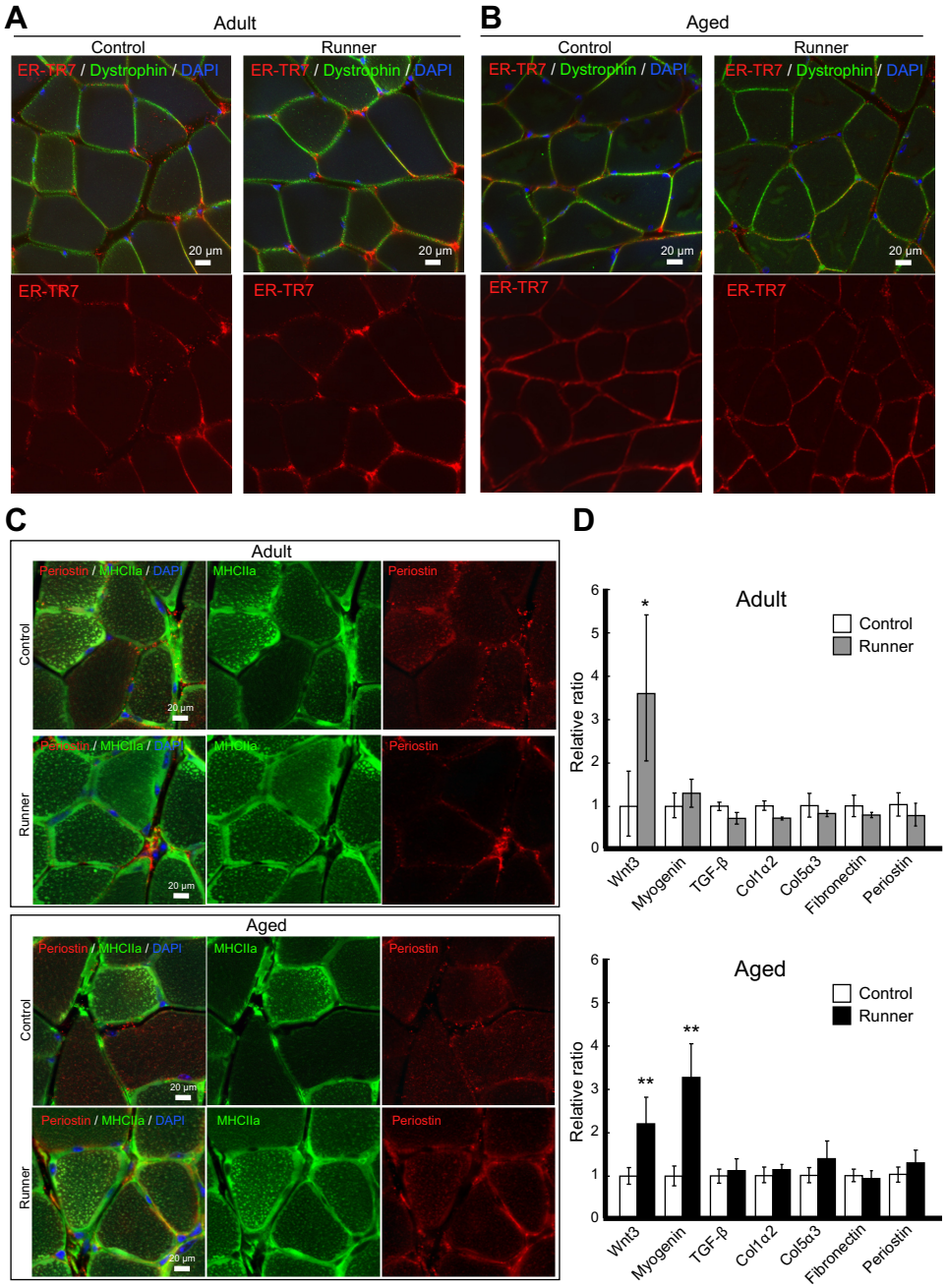

FIGURE 4. **Voluntary wheel running did not induce muscle fibrosis.** *A* and *B*, representative images of immunohistochemistry analysis of ER-TR7 (*red*) and dystrophin (*green*) in adult (*A*) and aged mice (*B*). *Left panels* are from the control group, and *right panels* are from the runner group. *C*, representative images of immunohistochemistry analysis of periostin (*red*) and MHC2a (*green*). The *upper panels* represent adult mice, and the *lower panels* represent aged mice (*upper panels* represent the control group, and *lower* represent the runner group, respectively). *D*, qRT-PCR analysis of *Wnt3*, myogenin (*Myog*), and fibrotic mRNAs (*TGF-β*, collagen 1α2 (*Col1α2*), collagen 5α3 (*Col5α3*), fibronectin (*Fn1*), and periostin (*Postn*)). The mRNA expression was normalized to that of GAPDH and then plotted as the expression ratio of each gene relative to the control sample in the adult group. *White bars*, controls in adult and aged mice; *gray bars*, adult runner mice; *black bars*, aged runner mice. All data are expressed as the mean ± S.D. ($n = 4$/group). Significant differences are as follows: *, compared with adult control group; **, compared with aged control group ($p < 0.05$). *Scale bars*, 20 μm in all panels.

3*B*). Upon phosphorylation of GSK-3β, high levels of accumulated β-catenin were detected in the skeletal muscles of mice that underwent exercise (Fig. 3*C*). Although recent studies have implicated Wnt signaling in abnormal repair and fibrogenesis (10), almost no stimulation of fibrosis was observed in runner group samples at both the mRNA and protein levels (Fig. 4).

To better understand the regulatory mechanisms linking the observed activation of the satellite cell population and the elevated Wnt signaling in runner group mice, we next tried to determine the direct target genes of the Wnt signaling pathway following voluntary wheel running. Because cooperative increases in the expression levels of Wnts, *Myf5*, and *MyoD* and the appearance of activated $Pax7^+Myf5^+$ and $Pax7^+MyoD^+$ satellite cells were observed, we simply examined whether the activator complex associated with canonical Wnt signaling bound the promoters of *MyoD* and *Myf5* genes. First, we investigated ~5 kb of the regulatory region upstream of the *Myf5* and *MyoD* genes of mice, rats, and humans. As shown in Fig. 5*A*, many consensus

sequences of the TCF/LEF regulatory element were present in the mouse, rat, and human *Myf5* promoter regions. Interestingly, a sequence (AACAAACAAA) containing multiple TCF/LEF regulatory elements and highly conserved in mice, rats, and humans was found 2.5 kb upstream in the *Myf5* promoter region (Fig. 5*A* and supplemental Fig. S1). Furthermore, a similar conserved sequence (ATTTCAAATTTTGC) was also found in the mouse, rat, and human *MyoD* promoters (supplemental Fig. S2). The conserved sequence 2.7 kb upstream of the *MyoD* gene involved the TCF/LEF regulatory element (Fig. 5*B*). These findings implied that Wnt signaling retained an indispensable role in the transcriptional regulation of the *Myf5* and *MyoD* genes.

ChIP-PCR analysis was performed to examine the effect of exercise-dependent increases in Wnt expression on the chromatin-mediated regulation of the *Myf5* and *MyoD* genes (Fig. 5, *C* and *D*). In the dissected skeletal muscle of adult runner mice, the association of HDAC1 with the TCF/LEF regulatory elements of the *Myf5* promoter decreased (>80%). In aged runner mice, the association of HDAC1 further decreased (>90%). A similar dissociation of HP1, a reader of repressive methylation at the level of histone H3 lysine 9, was detected on the *Myf5* promoter in adult and aged skeletal muscle. Histone methylation is known to be associated with both transcriptionally active and repressive chromatin states. The enrichment of dimethylated H3 lysine 9 (K9me2) on the *Myf5* promoter disappeared after exercise in both adult and aged mice, suggesting that a repressive chromatin state controlled the aged stage. In the dissected skeletal muscle of runner mice, dimethylated histone H3 K4 (K4me2) and acetylated histone H3 (Ac-H3), modified histones associated with gene activation, were apparently enriched on the *Myf5* promoter compared with those in control mice. The associations of β-catenin, LEF1, and TCF with the conserved regulatory sequences on the *Myf5* promoter were enriched upon voluntary exercise, indicating that the β-catenin·TCF·LEF-mediated activator complex associated in response to Wnt signaling.

Similar results were observed with *MyoD*. *MyoD* was expressed in activated satellite cells, as was *Myf5*, and both basic helix-loop-helix transcription factors retained similar epigenetic profiles following exercise, implying that running stimulation altered the chromatin structure of *MyoD* and *Myf5* genes, even in aged skeletal muscle. The enhancement of β-catenin·TCF·LEF binding to Wnt signaling regulatory sites on the *Myf5* promoter was higher than that of the *MyoD* promoter, suggesting that the binding efficiency reflected the structure of the six TCF/LEF regulatory sites on the mouse *Myf5* promoter and of the two TCF/LEF regulatory sites within the detection site used in our ChIP analysis. These results suggested that voluntary wheel running increased the *de novo* expression of *Wnt3* in adult and aged mice and thereby rescued impaired myogenesis in aged mice via the canonical Wnt signaling-mediated transcriptional activation of the *Myf5* and *MyoD* genes, important targets that drive the state of activated satellite cells. Associations of β-catenin, TCF, LEF1, K4me2, and Ac-H3 increased upon exercise, whereas K9me2, HDAC1, and HP1 were dissociated from the Wnt signaling response elements on the *Myf5* and *MyoD* promoters after exercise, suggesting that an active chromatin state controlled myogenesis in adult and aged skeletal muscle upon exercise. Taken together, these findings supported the conclusion that exercise stimulus-associated Wnt expression contributed to genetic chromatin reassembly in adult myogenesis rather than to fibrosis and promoted myogenic proliferation and exit from the quiescent states of satellite cells, which was critical for exercise-dependent myogenesis in adult and aged skeletal muscle.

DISCUSSION

In this study, we investigated the characteristic changes in satellite cells and the molecular mechanisms regulating their activation in mouse skeletal muscle following voluntary wheel running. Our analysis showed that exercise induced the up-regulation of several Wnts in myofibers (Fig. 3) and that activation of the canonical Wnt/β-catenin signaling pathway increased the expression of *Myf5* and *MyoD* in satellite cells (Fig. 2, *A–D*) through association of the β-catenin·TCF·LEF activator complex with the *Myf5* and *MyoD* promoters (Fig. 5). *Myf5* is expressed in only $Pax7^+$ cells, satellite cells but not in myofibers, and *MyoD* is also expressed in satellite cells or differentiating myoblasts (Fig. 2) (44). Therefore, we focused to assess the regulatory mechanism of *Myf5* and *MyoD* genes in skeletal muscle. In the case of adult neurogenesis, astrocyte cells residing near adult neural stem cells produce Wnt3 ligands (35) and the secreted extracellular Wnts trigger the neurogenesis by promoting the expression of NeuroD basic helix-loop-helix transcription factor (38, 39). Because Wnt3 expression in adult brain flexibly changes by responding to external stimuli such as running exercise (45), stem cell niches act as a sensor to modulate the ability of adult neural stem cells. In the case of adult skeletal muscle, a similar relationship between satellite cells (trigger myogenesis via the basic helix-loop-helix myogenenic genes) and residing myofibers (Wnt production) were observed in the current study. Wnt-mediated expression of myogenic genes in satellite cells caused their conversion from the quiescent state into the activated state in both adult and aged mice. Wnt signaling plays an important role in embryonic muscle development (7, 34). The neural tube expresses Wnt1, which activates the *Myf5* gene, whereas the dorsal ectoderm expresses Wnt7a, which promotes *MyoD* expression (46). Although Wnt retains its necessary role in muscle development during the embryonic stage (47, 48), it also contributes to postnatal/adult myogenesis in the muscle regeneration process after injury. In adult skeletal muscle, CTX-induced injury increases the expression of *Wnt5a*, *Wnt5b*, and *Wnt7a* mRNA, and the induction is accompanied by the generation of $Myf5^+$ cells (49). In a study using *in vitro* myoblast cultures, the up-regulation of myogenin and MHC, mature stage markers, was seen on treatment with lithium chloride (LiCl), a GSK-3β inhibitor that activates Wnt signaling (50). Treatment of myoblasts with Wnt3a also promoted the progression of differentiation accompanied by accelerated expression of desmin, a cytoskeletal intermediate filament protein (9). Our study demonstrated that the exercise-mediated activation of Wnt signaling affected satellite cells in the first step of adult myogenesis rather than lineage progression into the mature stage. The expression levels of Wnt3, Wnt5a, and Wnt5b increased upon voluntary wheel running. These findings indicated the critical role of Wnt proteins in

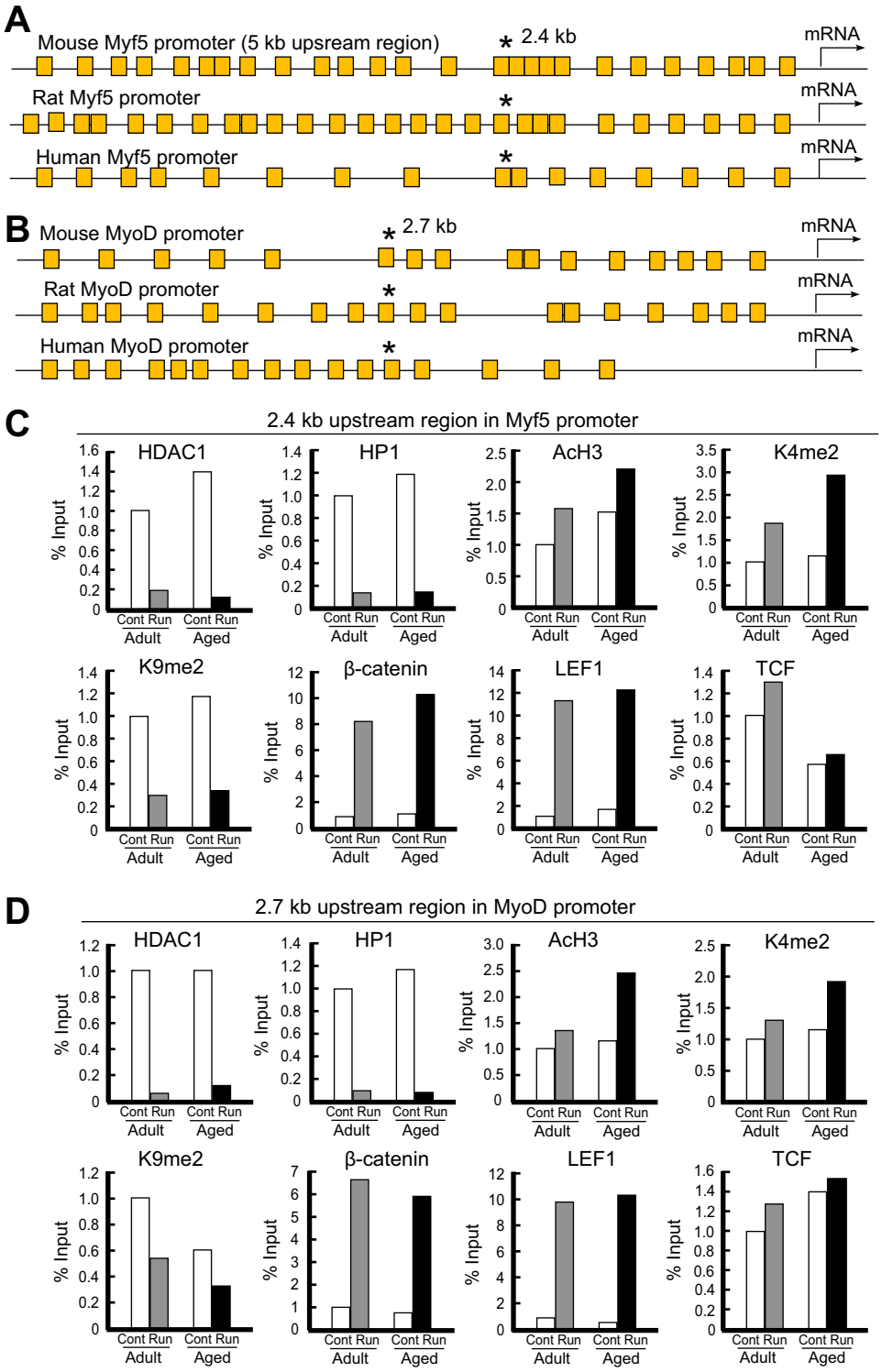

FIGURE 5. **Exercise-stimulated Wnt signaling directly triggered the expression of *Myf5* and *MyoD* transcripts in adult/aged skeletal muscle.** *A,* schematic representation of Wnt/β-catenin regulatory sites on the mouse, rat, and human *Myf5* promoters. The region about 5 kb upstream of the *Myf5* gene is shown with the TCF/LEF consensus sequence. Each *yellow square box* represents a TCF/LEF regulatory element. A highly conserved sequence within species (* indicates the location), AACAAACAAA, was located 2.5 kb upstream of the *Myf5* gene, and the conserved sequence contained multiple TCF/LEF regulatory elements. *B,* schematic representation of Wnt/β-catenin regulatory sites on the mouse, rat, and human *MyoD* promoters. The region about 5 kb upstream of the *MyoD* gene is shown with the TCF/LEF consensus sequence. A highly conserved sequence within species (* indicates the location), ATTTCAAATTTTGC, was located 2.7 kb upstream of the *MyoD* gene, and the conserved sequence involved the TCF/LEF regulatory element. *C,* ChIP analysis of the mouse *Myf5* promoter in adult/aged skeletal muscle after voluntary wheel running. PCR primers were designed to surround the TCF/LEF regulatory elements that are conserved within species at 2.5 kb upstream of the *Myf5* gene. ChIP results obtained by independent replicate experiments are represented as percentages of the input signal (signal relative to input (%)). Signals are represented by *white bars* (controls in adult and aged mice), *gray bars* (adult runner mice), and *black bars* (aged runner mice). *D,* ChIP analysis of the mouse *MyoD* promoter in adult/aged skeletal muscle after voluntary exercise. PCR primers were designed to surround the TCF/LEF regulatory element contained within the conserved sequence among mouse, rat, and human *MyoD* promoters at the 2.7-kb upstream locus.

adult myogenesis. Among the various Wnt proteins, specific isoforms are activated in response to different treatments (*e.g.* drugs, reagents, and ligands) and stimuli (*e.g.* exercise, injury, and surgery altering the serum environment); the signaling pathways also differ between canonical and noncanonical signaling.

The positive role of Wnt signaling in adult skeletal muscle differentiation under various types of exercise has been described in several recent studies. Acute treadmill running and functional overload decreases GSK-3β activity and activates canonical Wnt signaling in skeletal muscle (22). Following functional overload, β-catenin, frizzled receptor, and *LEF1* mRNA expression increased in the plantaris muscle (23). Moreover, the number of β-catenin-expressing M-cadherin-positive cells increases upon functional overload (51). These exercise types mimic the high intensity resistance exercise required for strengthening muscles. Acute high intensity exercises, such as jogging and running, cannot be performed easily, especially in aged individuals, where the risk of sarcopenia increases. In the case of voluntary wheel running, the exercise intensity is low and less stressful than that of other activities. Similar to a study in which high intensity exercise was enforced (22, 23), the voluntary wheel running used in this study as mild exercise up-regulated the expression of Wnt isoforms effectively in both adult and aged skeletal muscle.

However, in aged mice, the exercise-mediated up-regulation of Wnts and the activation of the canonical Wnt/β-catenin signaling pathway cannot be simply accepted as clinically beneficial because elevated Wnt signaling also stimulates fibrosis (10, 52). A previous parabiosis mouse study reported a decrease in GSK-3β and an increase in β-catenin and axin 2 (downstream targets of Wnt signaling), indicating that the up-regulation of Wnt signaling in aged mice induces fibrosis rather than triggering myogenic differentiation (10). Moreover, Brack *et al.* (10) reported that most of the satellite cells isolated from aged mice differentiate into fibroblasts, whereas those from young mice do not. Scimè *et al.* (53) reported that the expression of Wnt inhibitors, such as secreted frizzle-related protein 2 (sFRP2) and Wnt inhibitor factor 1 (Wif1), decreases with age, suggesting a decrease in Wnt antagonism during aging. These data suggest that increased Wnt signaling during aging potentially induces the transdifferentiation of satellite cells into a fibrogenic lineage. However, in this study, both IHC and qRT-PCR analyses showed that there were no differences in the levels of ER-TR7, periostin, or collagen 1 expression between adult and aged mice. ER-TR7 is a marker of reticular fibroblasts and reticular fibers and is generally used to detect fibrosis (10, 40). Periostin is a fibrotic protein retaining the role of critical regulator of fibrosis and is located in the extracellular matrix of skeletal muscle and fibroblasts (41). Knock-out of periostin suppresses muscular dystrophy-induced fibrosis (42). Importantly, although voluntary exercise induced significant up-regulation of Wnts and activation of the canonical Wnt/β-catenin signaling pathway in our study, in turn increasing the expression of the *Myf5* and *MyoD* myogenic genes, exercise-induced up-regulation of Wnt signaling was not involved in muscle fibrosis. Therefore, we can speculate the following: 1) exercise-responding Wnts inhibit fibrosis; 2) artificial surgery exposing the aged environment to young skeletal muscle may cause unexpected regulatory responses that do not reflect the normal action of Wnt and related molecules; and 3) other factor(s) co-exist to cause distinct phenotypes under canonical Wnt signaling depending on the physiological conditions (exercise *versus* inflammation, healthy subjects *versus* muscle dystrophy/disease, and low stress condition *versus* stressful condition).

In conclusion, this study revealed the regulatory mechanisms underlying Wnt-mediated myogenesis in satellite cells after exercise. The voluntary wheel running used in this study as mild exercise up-regulated canonical Wnt/β-catenin signaling in skeletal muscle. The expression levels of Wnt3, Wnt5a, and Wnt5b significantly increased after 4 weeks of voluntary running in both adult and aged mice, and the elevated Wnts and downstream signaling cascade did not induce fibrosis, even in aged skeletal muscle. The canonical Wnt/β-catenin signaling pathway directly modulated the chromatin structures of both the *MyoD* and *Myf5* genes and activated their expression at the transcriptional level. Exercise-stimulated chromatin remodeling on the *MyoD* and *Myf5* promoters altered the state of satellite cells from quiescent to activated, resulting in increased numbers of proliferative $Pax7^+MyoD^+$ cells. The associations of β-catenin, TCF, and LEF transcription factors on multiple TCF/LEF regulatory elements, conserved in mouse, rat, and human species, on the promoters of both the *Myf5* and *MyoD* genes drove myogenesis in satellite cells, even in aged muscle, suggesting that exercise-stimulated extracellular Wnts played a critical role in the regulation of satellite cells in adult and aged skeletal muscle. Our study suggested that mild running was effective in preventing the progression of sarcopenia because exercise-induced Wnts did not cause fibrosis in aged skeletal muscle and rescued the activity of satellite cells. Further studies aiming to discriminate between the effects of Wnts in the exercise state and fibrotic state and for determining the modulator(s) controlling signaling are crucial for understanding the functions and intrinsic ability of satellite cells in adult myogenesis.

Acknowledgments—We thank Hideto Takimoto and Kaori Naka for providing assistance with animal care.

REFERENCES

1. Kuang, S., and Rudnicki, M. A. (2008) The emerging biology of satellite cells and their therapeutic potential. *Trends Mol. Med.* **14,** 82–91
2. Chargé, S. B., and Rudnicki, M. A. (2004) Cellular and molecular regulation of muscle regeneration. *Physiol. Rev.* **84,** 209–238
3. Kadi, F., Schjerling, P., Andersen, L. L., Charifi, N., Madsen, J. L., Christensen, L. R., and Andersen, J. L. (2004) The effects of heavy resistance training and detraining on satellite cells in human skeletal muscles. *J. Physiol.* **558,** 1005–1012
4. Umnova, M. M., and Seene, T. P. (1991) The effect of increased functional load on the activation of satellite cells in the skeletal muscle of adult rats. *Int. J. Sports Med.* **12,** 501–504
5. Renault, V., Thornell, L. E., Eriksson, P. O., Butler-Browne, G., and Mouly, V. (2002) Regenerative potential of human skeletal muscle during aging. *Aging Cell* **1,** 132–139
6. Perdiguero, E., Sousa-Victor, P., Ballestar, E., and Muñoz-Cánoves, P. (2009) Epigenetic regulation of myogenesis. *Epigenetics* **4,** 541–550
7. von Maltzahn, J., Chang, N. C., Bentzinger, C. F., and Rudnicki, M. A. (2012) Wnt signaling in myogenesis. *Trends Cell Biol.* **22,** 602–609

8. Otto, A., Schmidt, C., Luke, G., Allen, S., Valasek, P., Muntoni, F., Lawrence-Watt, D., and Patel, K. (2008) Canonical Wnt signalling induces satellite-cell proliferation during adult skeletal muscle regeneration. *J. Cell Sci.* **121,** 2939–2950
9. Brack, A. S., Conboy, I. M., Conboy, M. J., Shen, J., and Rando, T. A. (2008) A temporal switch from Notch to Wnt signaling in muscle stem cells is necessary for normal adult myogenesis. *Cell Stem Cell* **2,** 50–59
10. Brack, A. S., Conboy, M. J., Roy, S., Lee, M., Kuo, C. J., Keller, C., and Rando, T. A. (2007) Increased Wnt signaling during aging alters muscle stem cell fate and increases fibrosis. *Science* **317,** 807–810
11. Trensz, F., Haroun, S., Cloutier, A., Richter, M. V., and Grenier, G. (2010) A muscle resident cell population promotes fibrosis in hindlimb skeletal muscles of mdx mice through the Wnt canonical pathway. *Am. J. Physiol. Cell Physiol.* **299,** C939–C947
12. Arthur, S. T., and Cooley, I. D. (2012) The effect of physiological stimuli on sarcopenia; impact of notch and Wnt signaling on impaired aged skeletal muscle repair. *Int. J. Biol. Sci.* **8,** 731–760
13. Tsivitse, S. (2010) Notch and Wnt signaling, physiological stimuli and postnatal myogenesis. *Int. J. Biol. Sci.* **6,** 268–281
14. De Bono, J. P., Adlam, D., Paterson, D. J., and Channon, K. M. (2006) Novel quantitative phenotypes of exercise training in mouse models. *Am. J. Physiol. Regul. Integr. Comp. Physiol.* **290,** R926–R934
15. Eikelboom, R., and Mills, R. (1988) A microanalysis of wheel running in male and female rats. *Physiol. Behav.* **43,** 625–630
16. Swallow, J. G., Koteja, P., Carter, P. A., and Garland, T. (2001) Food consumption and body composition in mice selected for high wheel-running activity. *J. Comp. Physiol. B.* **171,** 651–659
17. Swallow, J. G., Koteja, P., and Carter, P. A., and Garland, T. (1999) Artificial selection for increased wheel-running activity in house mice results in decreased body mass at maturity. *J. Exp. Biol.* **202,** 2513–2520
18. Lambert, M. I., and Noakes, T. D. (1990) Spontaneous running increases Vo2max and running performance in rats. *J. Appl. Physiol.* **68,** 400–403
19. Allen, D. L., Harrison, B. C., Maass, A., Bell, M. L., Byrnes, W. C., and Leinwand, L. A. (2001) Cardiac and skeletal muscle adaptations to voluntary wheel running in the mouse. *J. Appl. Physiol.* **90,** 1900–1908
20. Schultz, R. L., Kullman, E. L., Waters, R. P., Huang, H., Kirwan, J. P., Gerdes, A. M., and Swallow, J. G. (2013) Metabolic adaptations of skeletal muscle to voluntary wheel running exercise in hypertensive heart failure rats. *Physiol. Res.* **62,** 361–369
21. Smith, H. K., and Merry, T. L. (2012) Voluntary resistance wheel exercise during post-natal growth in rats enhances skeletal muscle satellite cell and myonuclear content at adulthood. *Acta Physiol.* **204,** 393–402
22. Aschenbach, W. G., Ho, R. C., Sakamoto, K., Fujii, N., Li, Y., Kim, Y. B., Hirshman, M. F., and Goodyear, L. J. (2006) Regulation of dishevelled and β-catenin in rat skeletal muscle: an alternative exercise-induced GSK-3β signaling pathway. *Am. J. Physiol. Endocrinol. Metab.* **291,** E152–E158
23. Armstrong, D. D., and Esser, K. A. (2005) Wnt/β-catenin signaling activates growth-control genes during overload-induced skeletal muscle hypertrophy. *Am. J. Physiol. Cell Physiol.* **289,** C853–C859
24. Ikeda, S., Kawamoto, H., Kasaoka, K., Hitomi, Y., Kizaki, T., Sankai, Y., Ohno, H., Haga, S., and Takemasa, T. (2006) Muscle type-specific response of PGC-1α and oxidative enzymes during voluntary wheel running in mouse skeletal muscle. *Acta Physiol.* **188,** 217–223
25. Machida, M., and Takemasa, T. (2010) Ibuprofen administration during endurance training cancels running-distance-dependent adaptations of skeletal muscle in mice. *J. Physiol. Pharmacol.* **61,** 559–563
26. Chapman, M. D., Keir, G., Petzold, A., and Thompson, E. J. (2006) Measurement of high affinity antibodies on antigen immunoblots. *J. Immunol. Methods* **310,** 62–66
27. Mayhew, D. L., Kim, J. S., Cross, J. M., Ferrando, A. A., and Bamman, M. M. (2009) Translational signaling responses preceding resistance training-mediated myofiber hypertrophy in young and old humans. *J. Appl. Physiol.* **107,** 1655–1662
28. Miyazaki, M., McCarthy, J. J., Fedele, M. J., and Esser, K. A. (2011) Early activation of mTORC1 signalling in response to mechanical overload is independent of phosphoinositide 3-kinase/Akt signalling. *J. Physiol.* **589,** 1831–1846
29. Liao, P., Zhou, J., Ji, L. L., and Zhang, Y. (2010) Eccentric contraction induces inflammatory responses in rat skeletal muscle: role of tumor necrosis factor-α. *Am. J. Physiol. Regul. Integr. Comp. Physiol.* **298,** R599–R607
30. Hamada, K., Vannier, E., Sacheck, J. M., Witsell, A. L., and Roubenoff, R. (2005) Senescence of human skeletal muscle impairs the local inflammatory cytokine response to acute eccentric exercise. *FASEB J.* **19,** 264–266
31. Ostrowski, K., Rohde, T., Asp, S., Schjerling, P., and Pedersen, B. K. (1999) Pro- and anti-inflammatory cytokine balance in strenuous exercise in humans. *J. Physiol.* **515,** 287–291
32. Allen, D. L., Uyenishi, J. J., Cleary, A. S., Mehan, R. S., Lindsay, S. F., and Reed, J. M. (2010) Calcineurin activates interleukin-6 transcription in mouse skeletal muscle *in vivo* and in C2C12 myotubes *in vitro*. *Am. J. Physiol. Regul. Integr. Comp. Physiol.* **298,** R198–R210
33. Smith, H. K., Maxwell, L., Rodgers, C. D., McKee, N. H., and Plyley, M. J. (2001) Exercise-enhanced satellite cell proliferation and new myonuclear accretion in rat skeletal muscle. *J. Appl. Physiol.* **90,** 1407–1414
34. Fujimaki, S., Machida, M., Hidaka, R., Asashima, M., Takemasa, T., and Kuwabara, T. (2013) Intrinsic ability of adult stem cell in skeletal muscle: an effective and replenishable resource to the establishment of pluripotent stem cells. *Stem Cells International* **2013,** 420164
35. Lie, D. C., Colamarino, S. A., Song, H. J., Désiré, L., Mira, H., Consiglio, A., Lein, E. S., Jessberger, S., Lansford, H., Dearie, A. R., and Gage, F. H. (2005) Wnt signalling regulates adult hippocampal neurogenesis. *Nature* **437,** 1370–1375
36. Cisternas, P., Henriquez, J. P., Brandan, E., and Inestrosa, N. C. (2013) Wnt signaling in skeletal muscle dynamics: myogenesis, neuromuscular synapse and fibrosis. *Mol. Neurobiol.* **49,** 574–589
37. Varela-Nallar, L., and Inestrosa, N. C. (2013) Wnt signaling in the regulation of adult hippocampal neurogenesis. *Front. Cell. Neurosci.* **7,** 100
38. Kuwabara, T., Hsieh, J., Muotri, A., Yeo, G., Warashina, M., Lie, D. C., Moore, L., Nakashima, K., Asashima, M., and Gage, F. H. (2009) Wnt-mediated activation of NeuroD1 and retro-elements during adult neurogenesis. *Nat. Neurosci.* **12,** 1097–1105
39. Kuwabara, T., Kagalwala, M. N., Onuma, Y., Ito, Y., Warashina, M., Terashima, K., Sanosaka, T., Nakashima, K., Gage, F. H., and Asashima, M. (2011) Insulin biosynthesis in neuronal progenitors derived from adult hippocampus and the olfactory bulb. *EMBO Mol. Med.* **3,** 742–754
40. Rafael-Fortney, J. A., Chimanji, N. S., Schill, K. E., Martin, C. D., Murray, J. D., Ganguly, R., Stangland, J. E., Tran, T., Xu, Y., Canan, B. D., Mays, T. A., Delfín, D. A., Janssen, P. M., and Raman, S. V. (2011) Early treatment with lisinopril and spironolactone preserves cardiac and skeletal muscle in Duchenne muscular dystrophy mice. *Circulation* **124,** 582–588
41. Marotta, M., Ruiz-Roig, C., Sarria, Y., Peiro, J. L., Nuñez, F., Ceron, J., Munell, F., and Roig-Quilis, M. (2009) Muscle genome-wide expression profiling during disease evolution in mdx mice. *Physiol. Genomics* **37,** 119–132
42. Lorts, A., Schwanekamp, J. A., Baudino, T. A., McNally, E. M., and Molkentin, J. D. (2012) Deletion of periostin reduces muscular dystrophy and fibrosis in mice by modulating the transforming growth factor-β pathway. *Proc. Natl. Acad. Sci. U.S.A.* **109,** 10978–10983
43. Katoh, M., and Katoh, M. (2007) WNT signaling pathway and stem cell signaling network. *Clin. Cancer Res.* **13,** 4042–4045
44. Yablonka-Reuveni, Z., Day, K., Vine, A., and Shefer, G. (2008) Defining the transcriptional signature of skeletal muscle stem cells. *J. Anim. Sci.* **86,** 207–216
45. Okamoto, M., Inoue, K., Iwamura, H., Terashima, K., Soya, H., Asashima, M., and Kuwabara, T. (2011) Reduction in paracrine Wnt3 factors during aging causes impaired adult neurogenesis. *FASEB J.* **25,** 3570–3582
46. Tajbakhsh, S., Borello, U., Vivarelli, E., Kelly, R., Papkoff, J., Duprez, D., Buckingham, M., and Cossu, G. (1998) Differential activation of Myf5 and MyoD by different Wnts in explants of mouse paraxial mesoderm and the later activation of myogenesis in the absence of Myf5. *Development* **125,** 4155–4162
47. Cossu, G., and Borello, U. (1999) Wnt signaling and the activation of myogenesis in mammals. *EMBO J.* **18,** 6867–6872
48. Ridgeway, A. G., Petropoulos, H., Wilton, S., and Skerjanc, I. S. (2000) Wnt signaling regulates the function of MyoD and myogenin. *J. Biol. Chem.* **275,** 32398–32405

49. Polesskaya, A., Seale, P., and Rudnicki, M. A. (2003) Wnt signaling induces the myogenic specification of resident $CD45^+$ adult stem cells during muscle regeneration. *Cell* **113,** 841–852
50. Rochat, A., Fernandez, A., Vandromme, M., Molès, J. P., Bouschet, T., Carnac, G., and Lamb, N. J. (2004) Insulin and Wnt1 pathways cooperate to induce reserve cell activation in differentiation and myotube hypertrophy. *Mol. Biol. Cell* **15,** 4544–4555
51. Ishido, M., Uda, M., Masuhara, M., and Kami, K. (2006) Alterations of M-cadherin, neural cell adhesion molecule and β-catenin expression in satellite cells during overload-induced skeletal muscle hypertrophy. *Acta Physiol.* **187,** 407–418
52. Serrano, A. L., and Muñoz-Cánoves, P. (2010) Regulation and dysregulation of fibrosis in skeletal muscle. *Exp. Cell Res.* **316,** 3050–3058
53. Scimè, A., Desrosiers, J., Trensz, F., Palidwor, G. A., Caron, A. Z., Andrade-Navarro, M. A., and Grenier, G. (2010) Transcriptional profiling of skeletal muscle reveals factors that are necessary to maintain satellite cell integrity during ageing. *Mech. Ageing Dev.* **131,** 9–20